

Intrinsic magnetic properties of $\text{NdFeAsO}_{0.9}\text{F}_{0.1}$ superconductor from local and global measurements

R. Prozorov,* M. E. Tillman, E. D. Mun, and P. C. Canfield

Ames Laboratory and Department of Physics & Astronomy, Iowa State University, Ames, IA 50011

(Dated: 13 May 2008)

Magneto-optical imaging was used to study the local magnetization in polycrystalline $\text{NdFeAsO}_{0.9}\text{F}_{0.1}$ (NFAOF). Individual crystallites up to $\sim 200 \times 100 \times 30 \mu\text{m}^3$ in size could be mapped at various temperatures. The in-grain, persistent current density is about $j \sim 10^5 \text{ A/cm}^2$ and the magnetic relaxation rate in a remanent state peaks at about $T_m \sim 38 \text{ K}$. By comparison with the total magnetization measured in a bar-shaped, dense, polycrystalline sample, we suggest that $\text{NdFeAsO}_{0.9}\text{F}_{0.1}$ is similar to a layered high- T_c , compound such as $\text{Bi}_2\text{Sr}_2\text{CaCu}_2\text{O}_{8+x}$ and exhibits a $3D \rightarrow 2D$ crossover in the vortex structure. The $2D$ Ginzburg parameter is about $G_i^{2D} \simeq 10^{-2}$ implying electromagnetic anisotropy as large as $\epsilon \sim 1/30$. Below T_m , the static and dynamic behaviors are consistent with collective pinning and creep.

PACS numbers: 74.25.Ha, 74.25.Sv, 74.25.Qt

The recently discovered rare earth iron oxyphosphates represent a new class of layered, high- T_c superconductors [1]. Rich chemistry allows for both electron and hole doping [2] as well as magnetism coexisting with, and possibly enhancing superconductivity. Unfortunately, the same rich chemistry makes growth difficult and, so far, only polycrystalline samples exist with the exception of a very recent report of Sm - based single crystals of sizes smaller than reported in this work [3]. $\text{NdFeAsO}_{0.9}\text{F}_{0.1}$ (NFAOF) with transition temperature exceeding 51 K was reported in Ref.[4]. This and related materials with Sm and Pr have the highest ambient pressure T_c values and are also interesting because of the possible interplay of the local moment of the rare earth and superconductivity. Predictions have been made for vortex melting similar to $\text{Bi}_2\text{Sr}_2\text{CaCu}_2\text{O}_{8+x}$ (BSCCO-2212) [5] and quantum critical behavior [6]. A recent NMR study favors nodal superconductivity [7], infrared ellipsometry suggests large electromagnetic anisotropy [8] and evidence of electromagnetic granularity has also been reported [9]. These observations prompt further investigation of similarities to high- T_c cuprates. So far, reported magnetic measurements are limited to indication of the transition temperature. In this Letter we present detailed magnetization measurements on both single crystallite and bulk, polycrystalline NFAOF. These results provide clear insight into the mesoscopic and macroscopic behavior of the superconducting mixed state. NFAOF exhibits fast non-monotonic magnetic relaxation of the vortex state that is strikingly similar to that associated with the $2D$ vortex melting found in BSCCO-2212, but NFAOF has much stronger interlayer coupling.

High pressure synthesis of samples with a nominal composition $\text{Nd}(\text{O}_{0.9}\text{F}_{0.1})\text{FeAs}$ was carried out in a cubic, multianvil apparatus, with an edge length of 19 mm from Rockland Research Corporation. Stoichiometric amounts of NdFe_3As_3 , Nd_2O_3 , NdF_3 and Nd were pressed into a pellet with mass of approximately 0.5 g

and placed inside of a BN crucible with an inner diameter of 5.5 mm. The synthesis was carried out at about 3.3 GPa. The temperature was increased over a period of one hour to 1350 – 1400 °C and held for 8 hours before being quenched to room temperature. The pressure was then released and the sample removed mechanically. More details of the synthesis and characterization will be found elsewhere [10]. The value of 10% F substitution is nominal, based on the initial stoichiometry of the pellet. The synthesis yields polycrystalline $\text{NdFeAsO}_{0.9}\text{F}_{0.1}$ samples that contain what appears to be plate-like single crystals as large as 300 μm . Whereas extraction of these crystallites is difficult, we could measure properties of individual crystals by using local magneto-optical imaging. Comparing our observation with data from conventional magnetometry, we are able to provide in-depth magnetic characterization of these new superconductors. For the measurements of total magnetic moment, a slab-like sample that showed best overall screening and trapping of the magnetic flux was selected by using magneto-optical imaging. *Quantum Design* MPMS magnetometer was used for the measurements of the total magnetic moment. Magneto-optical (MO) imaging was performed in a ^4He optical flow-type cryostat using Faraday rotation of polarized light in a Bi - doped iron-garnet film with in-plane magnetization [11]. The spatial resolution of the technique is about 3 μm with a sensitivity to magnetic field of about 1 G. The temporal resolution is about 30 msec.

We first examined morphological features visible in polarized-light and then establish the correspondence between these features and the observed local magnetic behavior. Figure 1 (a) shows the entire sample used in the comparative study. Figure 1 (b) shows the MO image in a 100 Oe applied magnetic field obtained after zero-field cooling (zfc). There is Meissner screening, better seen in the magnetic induction profile shown in the main frame of Fig. 1 taken along the line shown in

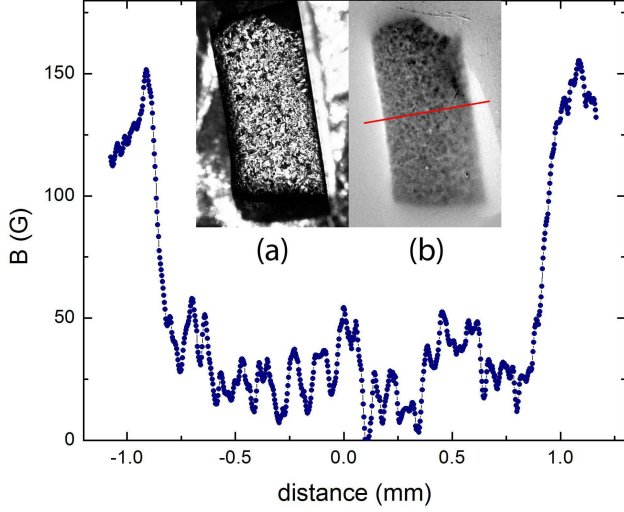


FIG. 1: Main frame: Meissner screening of a 100 Oe field applied after zfc. $B(r)$ was taken along the line shown in inset (b). Inset (a): Optical image of the sample used in magnetometry and local studies. Inset (b): MO image of a 100 Oe field applied after zfc.

Fig. 1 (b). Figures 2 (a) and (d) show two different regions of the polished sample and provide clear evidence of well - faceted crystallites with cross-sections as large as $200 \times 100 \mu m^2$. Sensitivity to the orientation of the light polarization plane with respect to the crystal structure serves as an additional indication that we are dealing with well ordered crystallites. Tetragonal symmetry of the unit cell suggests that the crystals should grow as plates with the ab - plane being the extended surface and the c - axis along the shortest dimension. We examined various cross-sections of the $\simeq 5$ mm diameter, 5 mm height pellets. Based on the thickness of extremely rectangular grains we estimate the thickness of the plates to be as large as $30 \mu m$. The magnetic flux penetration is consistent with isotropic in-plane persistent current densities, further confirming that the large grains represent the ab - plane of the tetragonal crystallites.

We can correlate this microstructure with the ability of this superconductor to shield magnetic field and trap the flux. Figure 2 (b) shows penetration of the magnetic flux into the region imaged in Fig. 2 (a) after zfc, whereas Fig. 2 (e) shows remanent (trapped) flux in the region imaged in Fig. 2 (d). Figures 2 (c) and (e) are the superpositions of Figs. 2 (a) and (b) and Figs. 2 (d) and (e), respectively. The correspondence between good superconducting regions and the largest crystals is evident.

There are several ways to estimate the shielding current from the measurements of total magnetic moment. For a slab of dimensions $2w \times 2b \times 2d$ (magnetic field is along the d side and $w \leq b$) within the Bean model

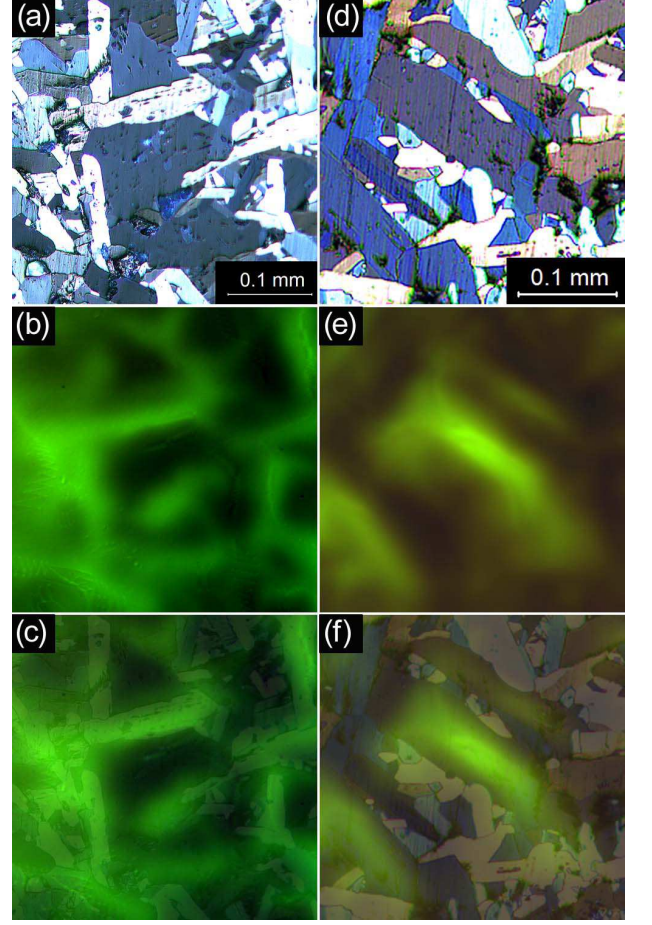


FIG. 2: (a) polarized-light image of part of the polished sample surface. (b) distribution of the magnetic induction upon penetration into the superconducting state, 550 Oe and 5 K is shown. (c) Superposition of (a) and (b). (d) - different part of polished surface. (e) remanent (trapped) flux after fc and turning field off. (f) Superposition of (d) and (e).

[12], total magnetic moment, M , is given by $M = jwV [1 - w/(3b)]/2c$ where, c is the speed of light, V is sample volume and j is the persistent (Bean) current that results from vortex pinning (we avoid calling this quantity "critical" current, because it is significantly affected by the magnetic relaxation). In the present case, for magnetic field parallel to the long side of a slab, $2d = 0.44$ cm, $2w = 0.07$ cm and $2b = 0.18$ cm and $V = 5.54 \times 10^{-3}$ cm³. Therefore, $j [A cm^{-2}] \simeq 1.2 \times 10^5 \times M [emu]$. Taking the maximum half-width of the full hysteresis loop, see inset to Fig.3, at $H = 0$, $M_{rem}(5 K) \simeq 0.2$ emu, we estimate $j(5 K) \simeq 2.4 \times 10^4 A cm^{-2}$. Another way to estimate shielding current density is to measure the field of full penetration [13], $H^* = 4wj(2 \arctan(\eta) + \eta \ln(1 + \eta^{-2}))/c$, where $\eta = d/w$. Field of full penetration may be estimated from the minimum of the $M(H)$ loop. In our case, we have $\eta = 6.3$, $H^* \simeq 1100$ Oe and therefore, $j \simeq 2.6 \times 10^4 A cm^{-2}$,

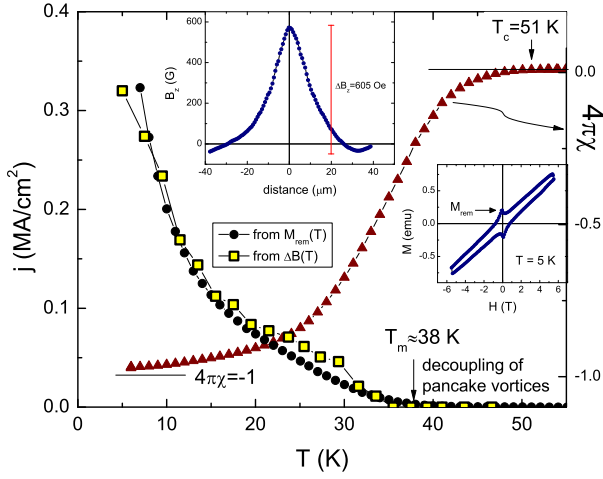


FIG. 3: Persistent current density, j , estimated from local MO measurements (see text). For comparison, $M_{rem}(T)$ is scaled to match the amplitude (circles). Also shown is $4\pi\chi$ (triangles, right axis) to emphasize the "magnetic" T_c . Upper inset shows example $B(r)$ and the definition of ΔB ; Lower inset shows an $M(H)$ loop at 5 K.

which is close to the above estimate and implies that superconducting fraction is close to 100 %. To verify this conclusion we measured reversible (Meissner) $M(H)$ at small, ± 10 Oe, field span which showed no hysteresis. The overall shielding was then estimated from $4\pi\chi = 4\pi(1 - N)M/VH$, where $N = (1 + 2\eta)^{-1} \simeq 7.4 \times 10^{-2}$ is the demagnetization factor (we neglected London penetration depth, λ , that enters via λ/w correction and thus irrelevant [14]). At 5 K we found, $4\pi\chi = -0.98$, essentially perfect diamagnetism. Given the uncertainty in V and N , as well as the neglected λ we see that this sample exhibits close to 100 % diamagnetic screening.

These results can be compared to local magnetic measurements. The persistent current may be evaluated from the measurements of the z - component of the magnetic induction on the slab's top surface using magneto-optical imaging. Defining $\Delta B = |B_z(x = 0, z = d) - B_z(x = w, z = d)|$ and assuming full critical state, we have [13]

$$\frac{\Delta B c}{4\tilde{j}\tilde{w}} = \eta \ln \frac{(1 + 4\eta^2)^2}{16\eta^3\sqrt{1 + \eta^2}} + 2 \arctan(2\eta) - \arctan(\eta)$$

where we use " \sim " to refer to quantities estimated for the individual crystallites. In the present case, a rectangular crystallite of $2\tilde{w} = 70 \mu\text{m}$, $2\tilde{b} = 160 \mu\text{m}$ and assuming thickness, $2\tilde{d} = 30 \mu\text{m}$, was analyzed. Therefore we have $\eta \simeq 30/70 \simeq 0.43$ and $\tilde{j} [\text{A cm}^{-2}] \simeq 529\Delta B [\text{G}]$. With $\Delta B \simeq 605$ we estimate $\tilde{j}(5 \text{ K}) \simeq 3.2 \times 10^5 \text{ A cm}^{-2}$. Clearly, there is about an order of magnitude difference with the estimate from bulk magnetization. The reason

is simple, - critical state is established in each individual crystallite, not on the scale of the entire sample, so and there is no macroscopic Bean gradient of the magnetic induction. This is why local measurement on the scale of an individual grain are required. Note that if $2\tilde{d}$ were infinite, the conversion would be $\tilde{j} \simeq 455\Delta B$, and for smaller $2\tilde{d}$ we expect larger conversion factor. Therefore, we provided the conservative estimate of the critical current.

Figure 3 summarizes *local* and global measurements of the persistent current density in NFAOF. Squares show $\tilde{j}(T)$ obtained from ΔB as defined in the upper inset. For comparison, full circles show the temperature dependence of the remanent magnetization rescaled by a single scaling factor to match the $\tilde{j}(T)$ obtained from local measurements. Suppose that the slab was split into crystallites of width $2\tilde{w}$ each carrying $\tilde{j} \sim 10^5 \text{ A cm}^{-2}$. A total of $n = w/\tilde{w}$ crystallites would produce a total magnetic moment of $\tilde{M} \sim n\tilde{j}\tilde{w}V \sim \tilde{j}\tilde{w}$. If we want this moment to match the observed M , then $\tilde{w} \sim wj/\tilde{j} \sim 0.1w$. With $w \simeq 350 \mu\text{m}$ we obtain a good agreement with the directly observed width of the crystallites, $\tilde{w} \sim 35 \mu\text{m}$. This yields an important conclusion - in our sample global magnetic measurements can be used to access intra-grain persistent current, but the estimated magnitudes will be about 10 times lower.

Figure 3 also shows other important features. The triangles (right axes) show magnetic susceptibility, $4\pi\chi$, measured at $H = 10$ Oe. The magnetic $T_c \simeq 51$ K and resistive $T_c \simeq 53$ K [10]. However, the $\tilde{j}(T)$ virtually vanishes above about 35 K. Remarkably, the order of magnitude and overall temperature dependence of $\tilde{j}(T)$ is quite similar to that observed in BSCCO-2212 [15] where there is a clear crossover above ~ 30 K associated with decoupling of pancake vortices ($3D \rightarrow 2D$ crossover) [16].

Given this last observation, we now turn to a discussion of the sample's dynamic properties. Magnetic relaxation is a valuable tool for determining vortex-related parameters of a superconductor [17, 18]. The relaxation rate depends on the pinning parameters as well as structure of the Abrikosov vortices and vortex lattice. A perfunctory inspection of the magnetic relaxation reveals a very large time dependence even at low temperatures. At 5 K, there is a 16% change of total magnetic moment over 1.5 h; there is even larger change of 38% at ~ 38 K. Whereas one can use sophisticated, nonlinear models, here it is sufficient to examine the logarithmic relaxation rate, $R = |d \ln M / d \ln t|$ which allows for comparison with other systems and is sample volume independent. Figure 4 shows a sharp increase of $R(T)$ and a peak at about ~ 38 K. It is worth noting that temperature of the peak is in the same temperature range that the apparent persistent current (Fig.3) drops almost to zero. Both observations are consistent with the vanishing of the barrier for vortex escape from the pinning potential at this tem-

perature.

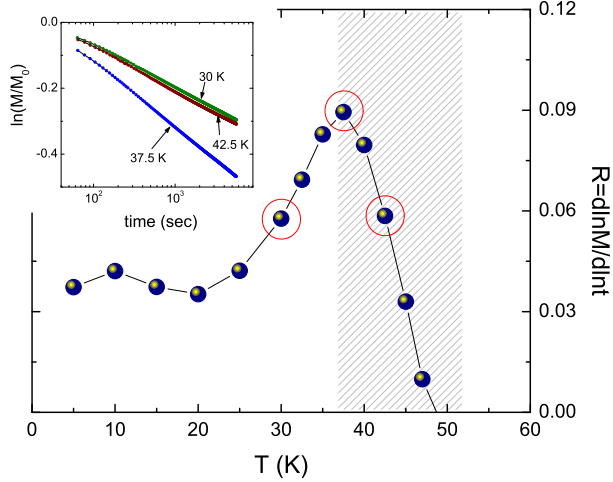


FIG. 4: Logarithmic relaxation rate $R = d \ln M / d \ln t$ as function of temperature. Shaded region shows anomalous behavior. Inset: time - dependent magnetization at three (circled) temperatures below, at and above the peak in $R(T)$.

Comparing to cuprate, high- T_c superconductors, we note that for different YBCO samples, including flux-grown, melt-processed crystals and films, $R(T)$ is confined to a narrow range between 0.02 and 0.04 and is fairly flat [18]. In contrast, for BSCCO, $R(T)$ exhibits a peak at temperature of a crossover associated with pancake decoupling [16, 18]. Examining the magnetic field dependence of the relaxation rate we find that below 38 K it drops very fast, despite the fact that the apparent irreversible magnetization is almost field independent above 1 kOe. This is consistent with the collective pinning and creep model in which the barrier for magnetic relaxation rapidly decreases with increasing magnetic field due to growth of vortex bundles.

The relaxation can also be measured in the individual crystallites. Figure 5 shows magnetic relaxation measured from a series of the snapshots taken initially at 150 msec intervals and later at 10 sec intervals. Examples of two such snapshots are shown as insets. To estimate the persistent current, profiles of magnetic induction, shown in the upper inset, were measured along the indicated path and then converted into j as described above. The relaxation rate is quite high, approaching $R = 0.1$, which reflects the fact that effective time constant depends on the sample size.

To understand our results from the point of view of unconventional, layered superconductors, we note that the overall, observed, magnetic behavior is similar to anisotropic high- T_c cuprates. Although without separate single crystals it is difficult to make firm conclusions, if we adopt the concept of a layered superconductor, then the dimensional crossover temperature signifies $2D$ melting, which, at zero field, is given

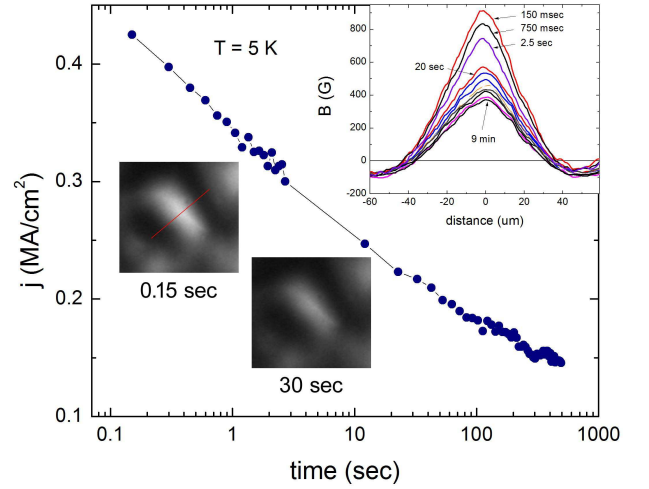


FIG. 5: Relaxation of the persistent current measured from the decay of the magnetic induction profiles shown in the upper inset. Embedded images show two frames at 0.15 sec and 30 sec after magnetic field was turned off. A line shows where profiles were taken.

by $T_m^{2D} = (T_{BKT}/4\sqrt{3}\pi) T_c / (T_c - T_{BKT})$ where T_{BKT} is Berezinskii-Kosterlitz-Thouless temperature [17]. In BSCCO-2212, $T_{BKT} \simeq 82$ K, $T_c \simeq 95$ K and $T_m^{2D} \simeq 28$ K. For NFAOF we therefore obtain, $T_{BKT} \simeq 48$ K with the observed $T_c \simeq 51$ K and $T_m^{2D} \simeq 38$ K. This lets us estimate the Ginzburg parameter, $Gi^{2D} \simeq (1 - T_{BKT}/T_c) v_s^\infty / 2\sqrt{2} \simeq 10^{-2}$ which is consistent with our assumption of a layered superconductivity ($v_s^\infty \simeq 0.5 - 0.9$ is the coupling renormalization [17]). This result implies a rather small penetration depth, $\lambda(0) < 100$ nm and electromagnetic anisotropy of the order of $\epsilon \sim 1/30$. These estimates will have to be refined when separate, single crystals are available.

In conclusion, we found evidence for a sharp crossover in the pinning mechanism at around $T_m^{2D} \approx 38$ K, which we interpret as a crossover from $3D$ Josephson coupled pancake vortices to decoupled $2D$ pancakes, similar to that found at ~ 30 K in BSCCO [16]. The temperature and field dependence of the persistent current as well as its logarithmic relaxation rate are consistent with collective pinning and creep [17, 18]. The estimated current density, $\sim 10^5$ A cm $^{-2}$ is low enough for weak collective pinning to hold. Overall, the behavior of NFAOF is somewhere in between YBCO and BSCCO.

Discussions with S. Bud'ko, V. Kogan, M. Tanatar, A. Kaminskii, W. McCallum, K. Dennis and J. Schmalian are greatly appreciated. Work at the Ames Laboratory was supported by the Department of Energy-Basic Energy Sciences under Contract No. DE-AC02-07CH11358. R. P. acknowledges support from NSF grant number DMR-05-53285 and the Alfred P. Sloan Foundation.

* Electronic address: prozorov@ameslab.gov

- [1] Y. Kamihara *et al.*, J. Am. Chem. Soc. **130** 3296 (2008).
- [2] Hai-Hu Wen *et al.*, Europhys. Lett. **82**, 17009 (2008).
- [3] N. D. Zhigadlo *et al.*, arXiv.org:0806.0337 (2008).
- [4] Z.-A. Ren *et al.*, arXiv.org:0803.4234 (2008).
- [5] J.-P. Lv and Q.-H. Chen, arXiv.org:0805.0632 (2008).
- [6] G. Giovannetti *et al.*, arXiv.org:0803.4234 (2008).
- [7] H. J. Grafe *et al.*, arXiv:0805.2595 (2008).
- [8] A. Dubroka *et al.*, arXiv:0805.2415 (2008).
- [9] A. Yamamoto *et al.*, arXiv:0805.1282 (2008).
- [10] M. Tillman *et al.*, in preparation (2008).
- [11] R. Prozorov, Phys. Rev. Lett. **98**, 257001 (2007)
- [12] C. P. Bean, Rev. Mod. Phys. **36**, 31 (1964).
- [13] R. Prozorov, Ph.D. thesis, *Bar-Ilan University* (1998).
- [14] R. Prozorov *et al.*, Phys. Rev. B **62**, 115 (2000).
- [15] R. Prozorov *et al.*, Phys. Rev. B **67**, 184501 (2003).
- [16] A. K. Pradhan *et al.*, Phys. Rev. B **49**, 12984 (1994).
- [17] G. Blatter *et al.*, Rev. Mod. Phys. **66**, 1125 (1994).
- [18] Y. Yeshurun *et al.*, Rev. Mod. Phys. **68**, 911 (1996).